Band-rejection filter based on spoof surface plasmon polaritons

BINGGANG XIAO*, JU LIANG, FENGLEI GUO
College of Information Engineering, China Jiliang University, Hangzhou, 310018, China

We propose a band-rejection filter based on the spoof surface plasmon polaritions (SPPs). The filter was designed by etching complementary single split-ring resonators (CSSRRs) on the waveguide for spoof surface plasmon polaritons (SPPs), which was made of periodic diamond hole array metal strips. A special transition structure basing on flaring ground and gradient hole was used to match the wave vector between coplanar waveguide (CPW) and Spoof SPPs waveguide. From dispersion relations, the structure of periodic diamond hole array metal strips can propagate the spoof SPPs waves when the operating frequency is no more than the cutoff frequency. The simulated results show the isolation of proposed filter can be less than -30 dB from 10.9 GHz to 12.1 GHz, and even reach to -30 dB from 11 GHz to 12 GHz. Due to the simple and compact structure, the proposed filter is easy to fabricate and integrate, which will have a broad application prospects in the follow-up developments of plasmonic integrated circuits and systems.

(Received July 28, 2017; accepted August 9, 2018)

Keywords: Band-rejection filter, Spoof surface plasmon polaritons, Split-ring resonators

1. Introduction

Surface plasmon polaritons (SPPs) are surface electromagnetic (EM) waves which occur at the interface of metal/dielectric and decay exponentially in the transverse direction at the optical frequency domain [1-2]. Due to the advantage of strong local-field enhancement, SPPs have attracted widespread research [2]. However, in the terahertz and microwave frequencies, the natural SPPs cannot be excited at metal/dielectric interface because of the perfectly electrical conductor (PEC) behavior of metal [2-4].

To overcome this problem, the plasmonic metamaterials of corrugated metal structures have been proposed to obtain strongly confined surface EM waves in the lower frequency regions, which are nowadays referred to as designer SPPs or spoof SPPs [5]. Since then, there have been many structures with periodic one-dimensional grooves or two-dimensional holes was reported to obtain such spoof SPPs [6-9]. In order to overcome the limitation of traditional 3D spoof SPPs structures in manufacture and integration, an ultrathin metal surface with periodical one-dimensional grooves was proposed by Cui et al, which has advantages of high field confinement, low transmission loss and easy integration in microwave circuit systems [10-12]. In recent years, the wide-band filters, band rejection filters, radiating antennas and some active devices have been produced successfully based on spoof SPPs, and it is evident that they will benefit to circuit integration and even system integration in view of the excellence of miniaturization and breaking the challenge of signal integrity [13].

In this work, we propose a band-rejection filter through etching single split-ring resonators (SSRRs) on the spoof SPPs planar holes structure. The SSRRs are etched on the metal part of the diamond hole arrays metal strips, coming into being complementary SSRRs (CSSRRs). A conventional coplanar waveguide (CPW) is used to connect system. A Special transition structure basing on flaring ground and gradient hole was used to smooth conversion between CPW and the spoof SPPs. We used the CST software to simulate and analyze the features of the filter. The simulated results show that the filter has a stop band from 10.9GHz to 12.1GHz and the simulated S_{21} of the stop band is less than -30dB. Compared to the conventional structure, such new structure is simpler and more compact. These features are significant for Spoof SPPs filter to apply in the follow-up developments of plasmonic microwave circuit system.

2. Proposed spoof SPPs waveguide

The proposed spoof SPPs waveguide is described in Fig. 1(a), which is formed by metal strip with periodic holes. The designed waveguide is printed on a dielectric substrate, whose relative dielectric constant is 4.3, loss angle is 0.003 and thickness is 0.065 mm. The thickness of the metal layer (annealed copper) is 0.018 mm. The Eigen-mode solver of commercial software, the CST Microwave Studio, is applied to analyze the dispersion relations of the spoof SPPs waveguide. Fig. 1(b) and Fig. 1(c) describe the dispersion relations of spoof SPPs with different physical dimensions. From Figures, we clearly observe that the behaviors of the curves are similar to SPPs. At low frequency, the dispersion curve of the spoof SPPs is close to the light line, and with the increases of the frequency, the wave vector of spoof SPPs deviate gradually from the light line. As is shown in Fig. 1(b), the cutoff frequency of the spoof SPPs decreases with the increases of the

structure width a. The cutoff of frequency for structure is 19.4 GHz when a = 0 mm, moving to 14GHz for the case of a = 2 mm. As is shown in Fig. 1(c), the cutoff frequency of the spoof SPPs becomes lower and lower with the increases of the length c. The cutoff frequency of the spoof SPPs is 21.5 GHz when b = 4 mm, while it move to 17.6 GHz when b = 5.8 mm. Obviously, the cutoff frequency of the structure is sensitive to the depth and the width of the hole. So the required cutoff frequency can be easily achieved by tuning the physical dimensions of the spoof SPPs structure.

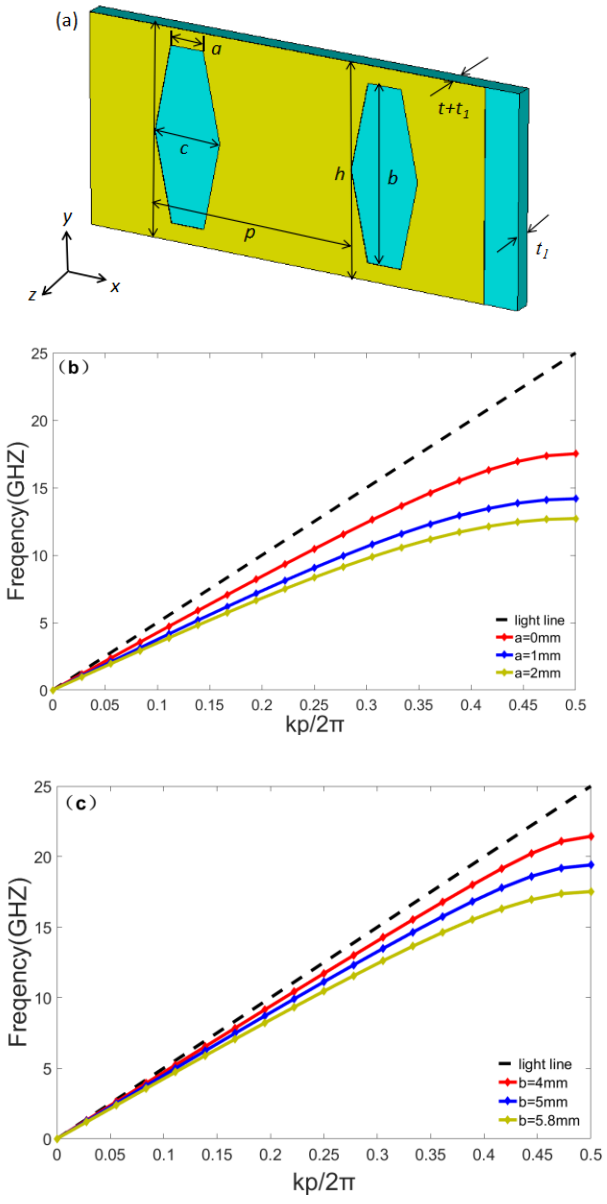

Fig. 1. (a) The schematic diagram of the proposed structure (b) Dispersion diagrams of the spoof SPPs waveguide with different hole width(a), in which b = 5.8mm, c = 2mm, p = 6mm, h = 6mm. (c) Dispersion diagrams of the spoof SPPs waveguide with different hole depths(b), in which a = 0mm, c = 2mm, p = 6mm, h = 6mm

3. Theory of CSSRRs

Complementary split-ring resonators (CSRRs) are a new type of metamaterials with negative permittivity [14-18], which have ability of inhibiting signal propagation in the vicinity of their resonance frequency [19-20]. Complementary single split-ring resonator (CSSRR) is customized version of conventional CSRR with single split-ring instead of two [21] and it exhibits the similar ability with CSRR. For above performances, these structures are widely used to exhibiting metamaterial properties in the design of microwave devices [20-22].

The characteristics of CSRR are analyzed in ref. 13, we mainly analyze and compare the performances of CSRR and CSSRR in this chapter. The geometries of CSRR and CSSRR we studied are shown in Fig. 2(a) and Fig. 2(b), where r is the radius of the structure. The CSRR and CSSRR are etched on the metal center between two holes. For the integrity of these structures, the radius of outer ring r should be less than the shortest length between two holes. To get a better understanding of the rejection property, the time-domain solver of commercial software-CST Microwave Studio was used to simulate the transmission coefficients of those structures with different sizes. Fig. 2(c) depicts the resonance frequencies of CSRR and CSSRR as a function of r when p = 6 mm, a = 2 mm, b = 5.8 mm, d = 6 mm, w = 0.35 mm, g = 0.15 mm and t = 0.018 mm. We can easily see the simulated relationship between resonant frequency and ring radius r that the resonant frequency of the CSRR decreases as the size of ring increases and the resonant frequency of CSSRR is higher than CSRR when they have the same physical dimensions. It implies that we can control the cutoff frequency of the band-rejection filter by turning the ring radius size of these structures. Fig. 2(d) and Fig. 2(e) show the S_{21} transmission coefficients for 1, 3, 5 and 7 ring resonators in the waveguide. As the number of ring resonator increase, the notch of reject band becoming more and more deep and wide when the number of ring resonator is no more than five. Due to the coupling effect between rings, the effect of frequency selectivity is sensitive to the number of CSSRR. Obviously, the CSSRR structure exhibits the stronger frequency selective when the number of ring resonator is five. Furthermore, the reject bandwidth of CSSRR is wider than CSRR when the number of ring resonator is more than one. Therefore, we can choose CSSRRs structure to achieve a wider and stronger broadband-frequency rejection.

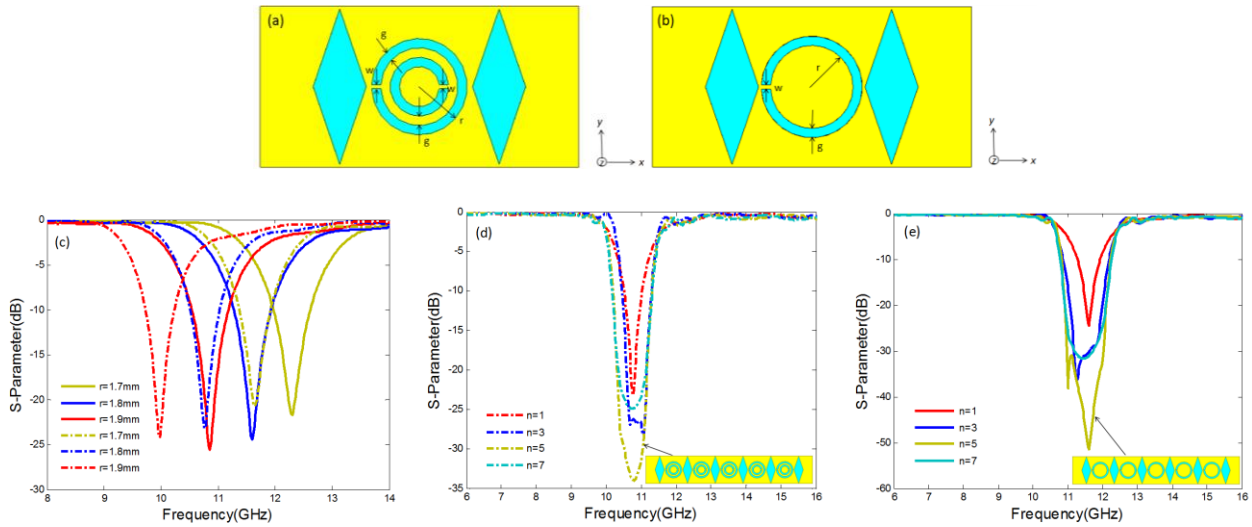

Fig. 2. (a) Schematic pictures of the CSRR structure. (b) Schematic pictures of the CSSRR structure. (c) The simulated transmission coefficients (S_{21}) of the circular CSRR and CSSRR with different ring radii. (d) and (e) The simulated transmission coefficients (S_{21}) of the CSRR and CSSRR with different number of ring resonator. (CSRR-Dashed line, CSSRR-Solid line)

4. Proposed filter

In order to improve the operating bandwidth and achieve a strongly broad rejection band, we use the CSSRR elements etched on the diamond hole arrays metal strips to design the band-rejection filter. The proposed band-rejection filter is depicted in Fig. 3, containing the diamond hole arrays metal strips, CSSRRs, CPWs and transition section. As shown in Fig. 3, the first part is CPW, which is designed to feed the guided-wave energies and receive the spoof SPPs signals. To achieve 50 Ω impendence, the parameters of CPW are chosen as H = 3 mm, s = 0.2 mm, and d = 15 mm. The parameters H is the half height of the central metal strip, d is the height of the flaring ground plane of CPW, and *s* is the gap between metal strip and flaring ground plane. The second part is special transition section, which serves as a bridge between the CPW and the SPP waveguide for impedance and momentum matching. The transition section contains gradient diamond holes and two flaring grounds. The curve of the flaring ground is governed by:

$$\begin{cases} y = C_1 e^{\alpha x} + C_2 \\ C_1 = \frac{y_2 - y_1}{e^{\alpha x_2} - e^{\alpha x_1}} \qquad (x_1 < x < x_2) \\ C_2 = \frac{y_2 e^{\alpha x_2} - y_1 e^{\alpha x_1}}{e^{\alpha x_2} - e^{\alpha x_1}} \end{cases} \tag{1}$$

where α = 0.2, (x_1,y_1) is the starting point of the curve and (x_2,y_2) is the ending point of the curve. The gradient diamond holes structure contain 10 gradient holes, and the depth of the hole is arithmetic decline from h_{10} = 5.8 mm to h_1 = 0.6 mm. The third part is the band-stop SPP waveguide, containing five same size CSSRRs etched on the diamond hole arrays metal strip. Here the parameters of CSSRR are chosen as r = 1.8 mm, w = 0.35 mm, g = 0.15 mm. The simulated S_{21} of band-rejection filter was shown in Fig. 4. It can be observed that the remarkable stop band from 10.9GHz to 12.1GHz, and the simulated S_{21} of the stop band is less than -30dB. It is clearly shown the good filtering performance of the band-rejection filter.

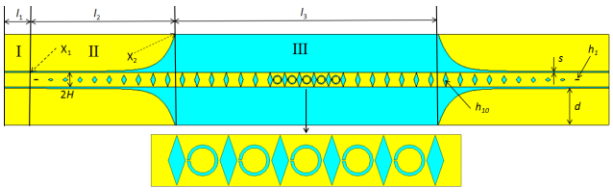

Fig. 3. Schematic pictures of the filter by etching CSSRR elements on the SPP transmission line, in which l_1 = 10 mm, l_2 = 60 mm, l_3 = 108 mm

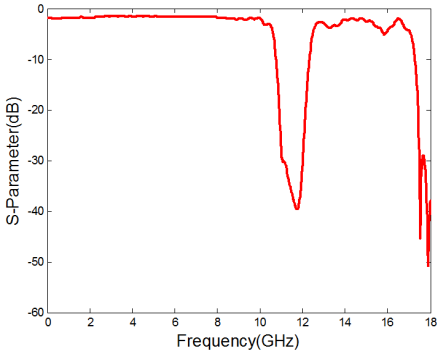

Fig. 4. The simulated transmission coefficients (S_{21}) of the proposed filter

5. Conclusion

In this work, we presented a band-rejection filter based on spoof SPPs. The CSSRRs have been etched on the spoof SPPs structure to provide signal propagation rejection at the vicinity of the resonance frequency. Due to the smooth conversion by using a special transition structure, the proposed filter has excellent transmission efficiency and low loss. The simulated results show that the proposed filter has more than 30dB rejections from 10.9GHz to 12.1GHz, demonstrating the highly efficient filtering performance. Owing to the excellent performance of low loss and high confinement, the proposed band-rejection filter will occupy an important position in the follow-up developments of plasmonic microwave circuit system.

Acknowledgments

This work was supported by 2016 Zhejiang Provincial Natural Science Foundation (grant number LY16F010010), in part by 2015 Zhejiang Province Public Welfare of International Cooperation Project (grant number 2015C34006).

References

[1] L. Liu, Z. Li, C. Q. Gu, et al., Appl. Phys. Lett. **116**, 58 (2014).
[2] J. Y. Yin, J. Ren, H. C. Zhang, et al., Sci. Rep. **5**, 8165 (2015).
[3] G. Kumar, A. Cui, S. Pandey, et al., Opt. Express **19**, 1072 (2011).
[4] H. F. Ma, X. Shen, Q. Cheng, et al., Laser & Photon. Rev. **110**, 146 (2013).
[5] B. C. Pan, Z. Liao, J. Zhao, T. J. Cui, Opt. Express **22**, 13940 (2014).
[6] P. Hibbins, B. R. Evans, J. R. Sambles, Science **308**, 670 (2005).
[7] D. Martin-Cano, M. L. Nesterov, A. L. Fernandez-Dominguez, et al., Opt. Express **18**, 754 (2010).
[8] X. Shen, T. J. Cui, Appl. Phys. Lett. **102**, 211909 (2013).
[9] Y. Zhang, P. Zhang, Z. J. Han, Lightwave Technol. **33**, 3796 (2015).
[10] J. J. Wu, D. J. Hou, T. J. Yang, et al., Electronics Letters **48**, 269 (2012).
[11] X. P. Shen, T. J. Cui, D. Martin-Cano, PNAS **110**, 40 (2013).
[12] D. Bao, X. P. Shen, T. J. Cui, Acta. Phys. Sin. **64**, 0228701 (2015).
[13] Q. Zhang, H. C. Zhang, J. Y. Yin, et al., Sci. Rep. **6**, 8256 (2016).
[14] P. Gaybalmaz, O. J. F. Martin, Journal of Applied Physics **92**(5), 2929 (2002).
[15] A. Abdel-Rahman, A. K. Verma, A. Boutejdar, et al., IEEE. Microw. Wireless. Compon. Lett. **14**, 36 (2004).
[16] J. S. Lim, C. S. Kim, D. Ahn, et al., IEEE Trans. Microw. Theory Tech. **53**, 2539 (2005).
[17] N. Katsarakis, T. Koschny, M. Kafesaki, et al., Applied Physics Letters **84**(15), 2943 (2004).
[18] J. D. Baena, J. Bonache, F. Martin, et al., IEEE Transactions on Microwave Theory & Techniques **53**(4), 1451 (2005).
[19] P. Gay-Balmaz, O. J. J. Martin, Appl. Phycol. **92**, 2929 (2002).
[20] J. Y. Deng, Y. Z. Yin, X. S. Ren, et al., J. Electromagnetic Wave **23**, 627 (2009).
[21] S. S. Kartikeyan, R. S. Kshetrimayam, IEICE. Electron. Express **7**, 1290 (2010).
[22] F. Aznar, J. Bonache, F. Martín, Applied Physics Letters **92**, 043512 (2008).

*Corresponding author: bgxiao@cjlu.edu.cn